

Time-optimal Control for Bilinear Nonnegative-in-control Systems: Application to Magnetic Manipulation ^{*}

Jiří Zemánek ^{*} Sergej Čelikovský ^{**} Zdeněk Hurák ^{*}

^{*} Faculty of Electrical Engineering, Czech Technical University in Prague, 12135 Prague, Czech Republic (e-mail: jiri.zemaneck@fel.cvut.cz, hurak@fel.cvut.cz).

^{**} Institute of Information Theory and Automation, Academy of Sciences of the Czech Republic, 18208 Prague, Czech Republic (e-mail: celikovs@utia.cas.cz)

Abstract: The paper describes a simple time-optimal control strategy for a class of second-order bilinear systems with nonnegative inputs. The structure of the model is motivated by the task of noncontact manipulation of an object in a planar force field generated by a single source; such setup constitutes a basic building block for a planar manipulation by an array of force field sources. The nonnegative-in-control property means that an object (particle) placed freely in the field can only feel an attractive force towards the source. In this paper we further restrict the control inputs to a binary signal—the field can be switched on and off. The control objective is to bring the object to the origin (where the source of the force field is located) as fast as possible. The optimal switching strategy is proposed using geometric arguments and verified using numerical simulations and experiments with a laboratory platform for noncontact magnetic manipulation.

Keywords: Bang-bang control, Bilinear systems, Mechatronics systems, Minimum-time control, Optimal control.

1. INTRODUCTION

1.1 Motivation—distributed planar manipulation of an iron ball through an array of coils

Before defining and solving an abstract control-theoretic problem, the ultimate engineering motivation is explained. As an alternative way of high-precision manipulation of objects in the plane, the concept of an actuator array has been introduced in the early 1990s by Böhringer et al. (1994). His further elaborations and contributions by his colleagues and followers were surveyed in Böhringer et al. (2000). The majority of that work was centered around open-loop control, intentionally avoiding sensors. Some later papers such as Luntz et al. (2001) and Murphey and Burdick (2004) suggested that a combination with feedback control may be needed in some situations, in particular when the actuator array is not dense enough. The authors of the current paper provided a survey in their paper Hurak and Zemanek (2012).

Unlike most of the above-referenced papers, the setting here is that although the set of actuators is discrete (forming a regular array), the resulting force field is (spatially) continuous. Notable practical instances of such force fields are electric and magnetic fields. These are often utilized for manipulation at micro- and nano-scales.

^{*} This research was funded by the Czech Science Foundation within the project P206/12/G014 (Centre for advanced bioanalytical technology, www.biocentex.cz) and the research grant No. 17-04682S.

In order to validate the theoretical findings of this paper, a laboratory experimental platform consisting of an array of coils was used. Although the platform is capable of continuous modulation of the currents through the coils, in the present paper a restriction is made on switching control—the current is either flowing or not. This is to investigate one practically important scenario—absence of electric current controllers would make similar platforms simpler. The experimental platform is shown in Fig. 1.



Fig. 1. The experimental platform consisting of a 4×4 array of coils with an iron core. A steel ball is placed on a resistive touch foil for real-time position measurement.

1.2 One-dimensional nonlinear model

A one-dimensional abstract scenario for the problem studied in this paper is in Fig.2.

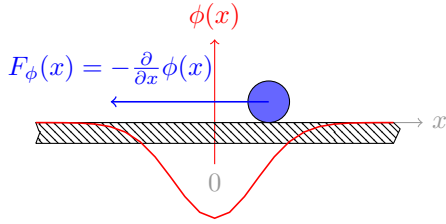


Fig. 2. One-dimensional restriction of the problem of manipulation by shaping a potential field through a single actuator.

Bell shape potential and the derived force field Force acting on the object is considered to be derived from the scalar potential that has an inverse bell shape. This is a practically reasonable assumption for actuators having spatially localized influence (e.g. electrodes, coils, etc.) As a simple example, we can consider a potential (magnetic pressure) of a magnetic monopole

$$\phi(x) = \frac{c}{2(x^2 + h^2)^2}, \quad (1)$$

where c comprises several physical parameters including the strength of the magnetic monopole and h is the vertical distance of the monopole from the horizontal plane of manipulation. The exerted force is then

$$F_\phi(x) = -\frac{\partial\phi(x)}{\partial x} = \frac{cx}{(x^2 + h^2)^3}. \quad (2)$$

Both the potential and the derived force (field) are shown in Fig.3 and they serve as a reasonable approximation for the application setup mentioned above, as we will demonstrate later in the paper. Besides, the inverse bell shape potential (namely Gaussian function) can be used to model a lateral force induced on a microparticle in a laser beam; a phenomenon exploited to create optical tweezers Gorman and Shapiro (2012). In fact, an extension of the proposed analysis into a plane, which would cover the domain of distributed planar manipulation, is the ultimate motivation for the research described in this paper.

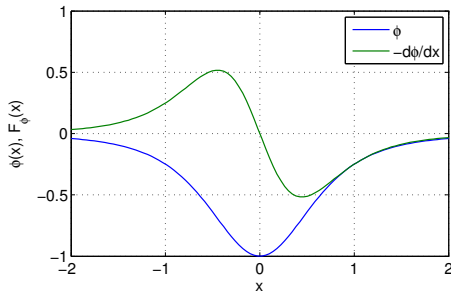


Fig. 3. The potential (magnetic pressure) and the force derived from it for a (virtual) magnetic monopole.

Equation of motion The equation of motion of a single object of mass m in the force field is

$$m\ddot{x}(t) = F_\phi(x, t) - F_{\text{friction}}(\dot{x}). \quad (3)$$

Apparently, an object initially located out of the origin will finally settle at the origin, but this settling process can be rather long and oscillatory if the friction is weak. This gives an incentive for finding a control scheme which steers the object to the origin faster. In the considered setup the friction is very small and ultimately will be neglected.

1.3 Bilinear model

Although the complete solution to the control problem must consider the full nonlinear model, the presented profile for the potential and force suggest that linear approximation is feasible in vicinity of the origin

$$m\ddot{x}(t) = -kx(t)u(t) - b\dot{x}(t), \quad u(t) \in \{0, 1\}, \quad (4)$$

where k represents a stiffness coefficient and b parameterizes the linear model of friction. The corresponding linear(ized) state-space model is

$$\begin{bmatrix} \dot{x}(t) \\ \dot{v}(t) \end{bmatrix} = \begin{bmatrix} 0 & 1 \\ 0 & -b/m \end{bmatrix} \begin{bmatrix} x(t) \\ v(t) \end{bmatrix} + \begin{bmatrix} 0 & 0 \\ -k/m & 0 \end{bmatrix} \begin{bmatrix} x(t) \\ v(t) \end{bmatrix} u(t), \quad (5)$$

$$u(t) \in \{0, 1\}.$$

This is an instance of a bilinear second-order model

$$\dot{\mathbf{x}}(t) = \mathbf{A}\mathbf{x}(t) + \mathbf{B}\mathbf{x}(t)u(t), \quad u(t) \in \{0, 1\}. \quad (6)$$

To make the structure of the model as transparent as possible, we introduce new real constants $\chi, \psi > 0$ and rewrite the state space model as

$$\begin{bmatrix} \dot{x}_1(t) \\ \dot{x}_2(t) \end{bmatrix} = \begin{bmatrix} 0 & 1 \\ 0 & -\chi \end{bmatrix} \begin{bmatrix} x_1(t) \\ x_2(t) \end{bmatrix} + \begin{bmatrix} 0 & 0 \\ -\psi & 0 \end{bmatrix} \begin{bmatrix} x_1(t) \\ x_2(t) \end{bmatrix} u(t), \quad (7)$$

$$u(t) \in \{0, 1\}.$$

For this model, a (switching) control will be designed. Finally, it is always possible to transform the system with $\psi \neq 1$ into a new one with $\psi = 1$ by introducing a new state and a time variable

$$\tilde{x}_1(\tilde{t}) = x_1(t), \quad \tilde{x}_2(\tilde{t}) = \frac{x_2(t)}{\sqrt{\psi}}, \quad \tilde{t} = t\sqrt{\psi}. \quad (8)$$

2. CONTROL STRATEGY

Our aim is to bring the object to the position $x_1(t) = 0$ with the velocity $x_2(t) = 0$ in the shortest time.

2.1 Indirect approach to optimal control

It is well known that the time-optimal control for constrained linear systems enforces the *bang-bang* control strategy, that is, the control signal is switched between two extreme values. Perhaps something similar can be

expected here and in our first attempt to solve the problem we ignore the discrete-valued (in fact, binary) character of the control signal and pretend that it can assume any real value within some bounds.

First, we consider the task of designing a control $u(t)$ that regulates the second-order nonlinear system. Hence the assignment is: bring the system described by

$$\dot{\mathbf{x}}(t) = \mathbf{A}\mathbf{x}(t) + \mathbf{F}(\mathbf{x})u(t), \quad u(t) \in [0, 1] \quad (9)$$

from any initial state to the state $(x_1(T), x_2(T)) = (0, 0)$ as fast as possible, that is, minimizing T .

The Hamiltonian (using the control-theoretic convention) for the minimum-time problem is

$$H(x, u, \lambda) = 1 + \boldsymbol{\lambda}^T(t) [\mathbf{A}\mathbf{x}(t) + \mathbf{F}(\mathbf{x})u(t)]. \quad (10)$$

Realizing that matrix $\mathbf{F}(\mathbf{x})$ is zero at the origin because there is no force exerted on the object there, that is,

$$\mathbf{F}(\mathbf{0}) = \mathbf{0}, \quad (11)$$

we observe that one of the necessary conditions of the minimum-time optimality, namely

$$H(T) = 0 \quad (12)$$

(see, for instance, Lewis and Syrmos (1995)) is impossible to satisfy because

$$H(T) = 1 + \underbrace{\boldsymbol{\lambda}^T(T)\mathbf{F}(\mathbf{0})u(T)}_{=0} = 1 \neq 0. \quad (13)$$

Obviously, the problem here is that the system is not controllable in the origin.

What to do then? We could possibly relax the requirement that $\mathbf{x}(T) = \mathbf{0}$ and penalize the deviation of the state \mathbf{x} from $\mathbf{0}$ by including the $\varphi(\mathbf{x}(T))$ term penalizing the final state in the cost function. A common choice is $\varphi(\mathbf{x}) = s\mathbf{x}^2(T)$. The boundary condition (12) will be replaced by the general condition

$$(\nabla_x \varphi - \boldsymbol{\lambda})^T \Big|_T d\mathbf{x}(T) + H|_T dT = 0. \quad (14)$$

Now what? The final state $\mathbf{x}(T)$ and the final time T (and hence their differentials) are independent anyway in this particular situation and therefore we can easily consider two independent conditions and we are back in the same troubles as before.

Note that approximating the nonlinear term $\mathbf{F}(\mathbf{x})$ in the vicinity of $\mathbf{x} = \mathbf{0}$ by a linear term $\mathbf{B}\mathbf{x}$ does not make the problem better approachable. Even here, pursuing the indirect approach apparently calls for some more advanced concepts from the domain of bilinear systems. These have been investigated, see Elliott (2009), for example. But the results are far from trivial. We have not pursued it any further in this work.

2.2 Direct approach—numerical optimal control

Rather than handling the boundary value problem generated by the first-order conditions of optimality as described in the previous section, the *direct approaches* are based on discretizing the time axis and reformulating the optimal control problem as an instance of nonlinear programming. Among the popular references are Betts

(2009), Diehl (2011) and Hargraves and Paris (1987). These numerical approaches provide an optimal trajectory as their outcome. It is then necessary to design a feedback controller that will steer the system along the trajectory. We have not pursued the approach here.

2.3 Geometric approach—Two switching lines, one aligned with the vertical axis

Since the control signal is constrained to assume one of two values (switched on and switched off), the techniques from the discipline of switching control might be invoked. Although there is a formal and rigorous framework for control of switched systems Liberzon (2003), Sun (2005), in this paper, we resort to simple and intuitive geometric arguments to arrive at a time-optimal solution.

There are two assumptions for the following development, though. We assume that the friction is negligible. With a steel ball rolling on a hard surface this seems to be a fair assumption as the damping is almost unnoticeable (frankly speaking, one does observe some damping during an operation, but it is of electromagnetic origin—eddy currents in the steel ball as it moves through the magnetic field). The second assumption or restriction is that we only consider regulation in the vicinity of the origin, where a bilinear model of the system applies. Making the controller work for a wider range, it seems inevitable to resort to some numerical optimal control methods.

The two state portraits for the switched-on and switched-off are shown in Fig.4; both portraits were generated for $\chi = 0$ and $\psi = 1$. The state portrait in Fig. 4(a) confirms a single invariant direction (eigenvector of $\begin{bmatrix} 0 & 1 \\ 0 & 0 \end{bmatrix}$), namely $v = [1 \ 0]^T$ corresponding to $\lambda = 0$. The state portrait in Fig. 4(b) confirms that there is no invariant direction for the state matrix $\begin{bmatrix} 0 & 1 \\ -1 & 0 \end{bmatrix}$ (no real eigenvector) and the state trajectory for the force field switched on keeps orbiting around the origin; obviously, without any control the force field will never steer the system asymptotically to the origin. The following control strategy is proposed.

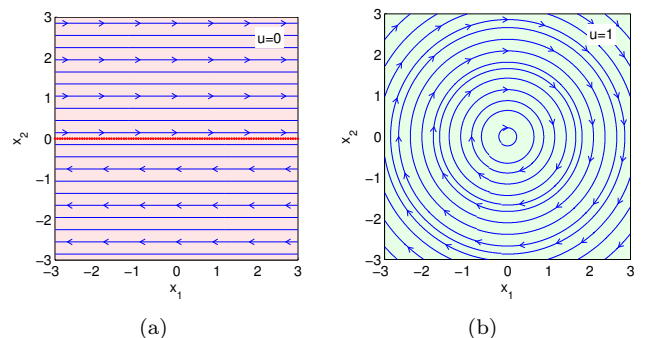


Fig. 4. State portraits for the field switched on and off. (a) State portrait for $u(t) = 0$. Single real eigenvector (corresponding to the zero eigenvalue) showed. (b) State portrait for $u(t) = 1$. No real eigenvector.

Two switching curves are used: a line with a (descending) slope given by a constant parameter $\gamma > 0$, that is

$x_2 = -\gamma x_1$, and the vertical axis, that is $x_1 = 0$. The justification for fixing the latter to the vertical axis will be given later. These two lines split the plane into four segments. The proposed controller switches the force field off and on when the state vector is in the upper right and lower left segment, since this is the only opportunity to bring the system closer to the origin. Invoking the concept of a switching function, the control is given analytically as

$$u(t) = \begin{cases} 1 & \text{if } \underbrace{\gamma x_1^2(t) + x_1(t)x_2(t)}_{s(t)} > 0, \\ 0 & \text{else,} \end{cases} \quad (15)$$

where the switching function $s(t)$ is indicated. The inequality $s(t) > 0$ is just a compact expression for

$$\begin{aligned} x_2(t) &> -\gamma x_1(t) \text{ if } x_1(t) > 0 \quad \text{or} \\ x_2(t) &< -\gamma x_1(t) \text{ if } x_1(t) < 0. \end{aligned} \quad (16)$$

To get some initial insight, we will arbitrarily choose $\gamma = \tan(\pi/6) \approx 0.5774$, that is, the switching line is at the angle of $\pi/6$ with the horizontal axis. For this particular value $\sin(\pi/6) = 1/2$, the norm $\|\mathbf{x}\|_2$ of the error is halved at every switching cycle, which makes the convergence analysis convenient. The analysis will be even more convenient while looking at the state portrait with the switching control in Fig. 5. Apparently, the state trajectory consists of a sequence of circular arcs and horizontal linear segments. It is possible to find an upper bound on the time needed to halve the initial velocity. Such time interval is given by three components

$$\tau_{1/2} = \frac{\pi}{2} + \pi/6 + \sqrt{3}, \quad (17)$$

where the first component is the time needed to travel through the upper right quadrant with the force field switched on; hence it constitutes an upper bound on the time needed to get from an initial state somewhere in the upper right quadrant to reach the horizontal axis. The second component is exactly the time required to travel along the circular arc of $\pi/6$ from the horizontal axis to the switching line. The last component is the time needed to travel along the horizontal line in the absence of force field. It comes from the observation that the length of the segment is $d \cos(\pi/6)$ and the constant velocity is $d/2$. It can also be written as $\cot(\pi/6)$.

For an arbitrary switching angle α (to which the controller parameter γ corresponds), an estimate of the upper bound of the time needed to reduce the norm of the regulation error to a given amount, say, to one half, possibly by taking multiple rounds (oscillation periods), is

$$\tau_{1/2} = \frac{(\frac{\pi}{2} + \alpha + \cot(\alpha))}{\log_{1/2}(\sin(\alpha))} = \ln(1/2) \frac{(\frac{\pi}{2} + \alpha + \cot(\alpha))}{\ln(\sin(\alpha))}. \quad (18)$$

The dependence of the time needed to halve the regulation error on the switching angle is in Fig. 6, including the optimal angle of 0.2433.

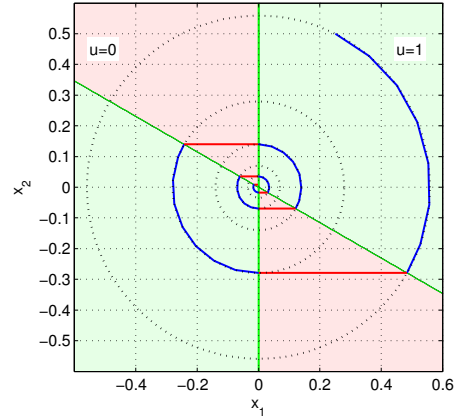


Fig. 5. $x_1(t)$ versus $x_2(t)$ in response to $x_1(0) = 1/4$ and $x_2(0) = 1/2$ for $\gamma = \tan(\pi/6) \approx 0.5774$ and no friction. The red segments of the state trajectory correspond to the field switched off. The two green lines are the switching curves.

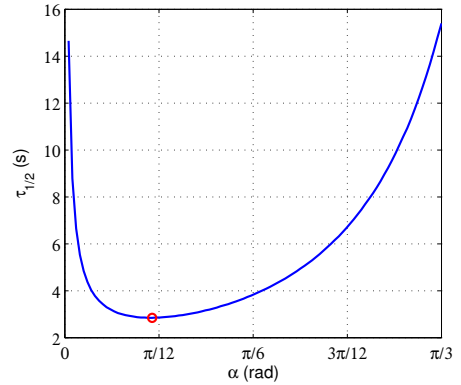


Fig. 6. Time to halve the initial norm of the error as a function of the switching angle α .

It is worth emphasizing that the above-given estimate is only approximate because the reduction of the error is only achieved during a portion of each cycle. This may be more pronounced if the needed number of cycles is small, which is actually the case in our application. This constitutes a challenge to be addressed in future.

A response of the system with an optimal controller to some nonzero initial conditions is in Fig. 7. The threshold δ mentioned in the figure will be addressed below.

2.4 Steady-state error analysis

Observe in Fig. 7 that $u(t)$ stops assuming the value 0 after some time, the field remains switched on. This is purely determined by the threshold parameter $-\delta$ substituted for zero on the right-hand side of the inequality in (15). The particular setting in Fig. 7 was $\delta = 10^{-6}$.

To get some insight into the constraint

$$\gamma x_1^2(t) + x_1(t)x_2(t) > -\delta, \quad (19)$$

consider $\delta = 10^{-1}$ and plot the approximate switching curve in Fig. 8. It is given by

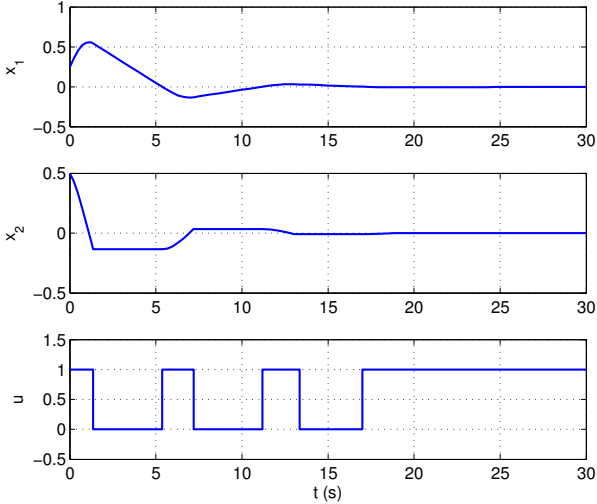


Fig. 7. $x_1(t)$ and $x_2(t)$ versus time in response to $x_1(0) = 1/4$ and $x_2(0) = 1/2$ for the optimal controller parameter $\gamma \approx 0.2493$ and the threshold $\delta = 10^{-6}$.

$$x_2(t) = \frac{-\delta}{x_1(t)} - \gamma x_1(t). \quad (20)$$

The curve is denoted approximate because the switching angles are not constant; the closer the system is to the origin, the more they move away from the optimal values. Finding the point on the curve closest to the origin we get the bound on the norm of the error

$$\|\mathbf{x}\|_2 < \sqrt{\frac{2\delta^2}{\sqrt{\frac{\delta^2}{\gamma^2+1}} - 2\delta\gamma}}. \quad (21)$$

With $\delta = 10^{-1}$ and $\gamma = 1/2$, the bound on the steady state error is 0.18, as evidenced in Fig. 8.

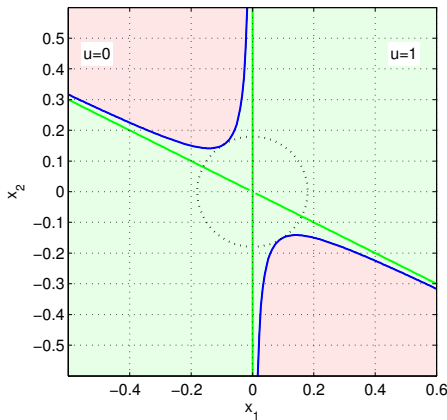


Fig. 8. Approximations (blue) of the switching curves (green) for the threshold $\delta = 10^{-1}$.

2.5 Can we improve on the regulation time by changing the switching angles from cycle to cycle?

The times needed for traveling along the arcs are independent of the radius, they only depend on the angle—Both the traveled distance and the velocity are proportional to the radius. The same holds for the horizontal paths. Hence,

the above computed optimal angle indeed guarantees optimality for the proposed switching scheme.

2.6 Can relaxing the condition on alignment of one of the switching lines with the vertical axis help improve the regulation time?

The control strategy introduced in the previous section was derived by fixing the controller structure (the number of switching curves set to two, one of them aligned to the vertical axis) first and then by optimizing over the single switching angle γ . It is not obvious, however, if by restricting to this particular controller structure, the optimal control strategy (among all possible switching control strategies) has been found. This section and the next gives an analysis. We address the question of relaxing the alignment of one of the two switching lines to the vertical axis first. Apparently, it only makes sense to switch the force field on and off in the upper left and bottom right quadrants in order to achieve a reduction in the regulation error. Due to symmetry, we will only conduct the analysis for the bottom right quadrant.

Consider an elementary *reduction step* as in Fig. 9. It is parameterized by the start angle α , which determines the instance the field is switched off, and the final angle β , which determines when the field is switched on again.

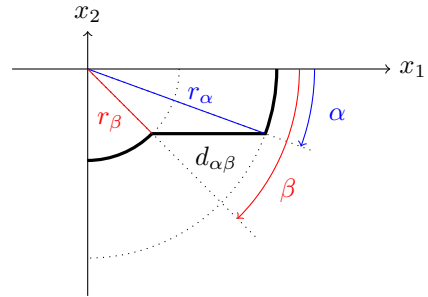


Fig. 9. Geometry of the elementary step towards reduction of the norm of the regulation error (distance from the origin, radius).

Following the style of analysis in the fixed $\beta = \frac{\pi}{2}$ case, the relative reduction of the radius (error) $r_{\alpha\beta}$ during one step (cycle) of reduction can be obtained as

$$r_{\alpha\beta} := \frac{r_\beta}{r_\alpha} = \frac{\sin(\alpha)}{\sin(\beta)}. \quad (22)$$

The constant-velocity part $d_{\alpha\beta}$ of the trajectory traveled by the object is

$$d_{\alpha\beta} = r_\alpha \cos(\alpha) - r_\beta \cos(\beta). \quad (23)$$

Thus the time $t_{\alpha\beta}$ needed for traveling along this constant-velocity segment is

$$t_{\alpha\beta} = \frac{d_{\alpha\beta}}{r_\alpha \sin(\alpha)} = \cot(\alpha) - \cot(\beta). \quad (24)$$

The total time needed to reduce the regulation error to 1/2 of the original value is given by

$$\begin{aligned}\tau_{1/2} &= \frac{\frac{\pi}{2} + \alpha + \cot(\alpha) - \cot(\beta) + (\frac{\pi}{2} - \beta)}{\log_{1/2}\left(\sin\left(\frac{\alpha}{\beta}\right)\right)} \\ &= \ln(1/2) \frac{\pi + \alpha + \cot(\alpha) - \cot(\beta) - \beta}{\ln\left(\sin\left(\frac{\alpha}{\beta}\right)\right)}.\end{aligned}\quad (25)$$

The above is a nonlinear function of two variables α and β , which are constrained as $0 \leq \alpha \leq \beta \leq \frac{\pi}{2}$. Graph of the function for a subset of the domain is in Fig. 10.

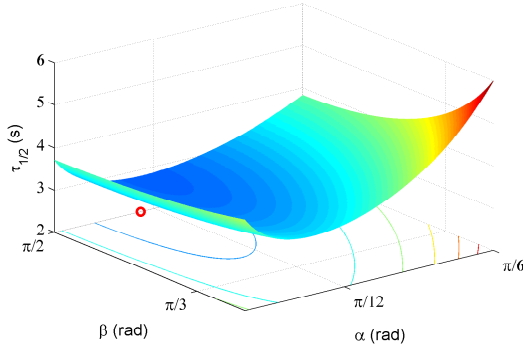


Fig. 10. Time to halve the regulation error as a function of the switching angles α and β .

By inspecting the graph, it can be seen that for a given α , the optimal β is on the boundary, that is, $\beta_{\text{optimal}} = \frac{\pi}{2}$.

2.7 Can multiple switching within one cycle improve the performance?

An analysis can go on to check if by allowing for switching on and off multiple times leads towards further reduction of the regulation time. Here we conjecture that the optimal strategy requires switching on and off exactly once in each cycle but a full proof will only be included in the extended version of the paper.

3. EXPERIMENTS

3.1 Platform

Experimental investigation of the performance of the presented control scheme was done using our custom-made laboratory apparatus for magnetic manipulation (Mag-Man). This magnetic platform consists of an array of 4×4 coils (grid 25 mm). Each coil is individually controlled—both the polarity and the amplitude of the current can be controlled. Therefore, it is possible to shape the magnetic field above the coils and use it for controlled manipulation with a magnetic object. In this case, a steel ball (radius 15 mm) for ball bearings serves as an object for manipulation. Although this platform allows proportional control of all coils, in the experiments conducted to support the theoretical findings of this paper, only on-off control of a single coil is used.

Commands are sent from the computer to the platform and the position of the ball is measured using a resistive touch foil (used typically for handheld devices with touch screens). The foil consists of two separated resistive flexible films which can be locally short-circuited at the point of

touch. This allows for measurement of voltage drop along the x and y directions. This, in turn, allows for calculation of the position of the ball. The foil is connected to the computer using a standard data-acquisition card. The computational power needed to estimate the position is negligible compared to the more popular computer vision based solution. Therefore, a high sampling rate can be easily achieved—in our case the controller runs at 1 kHz.

The platform was presented and awarded the first place in 2013 Matlab and Simulink design challenge http://youtu.be/AhS_2gU1qW0.

3.2 Mathematical model

The magnetic field created by the single coil in the horizontal plane above the coils can be in our case approximated by the magnetic field created by a simple magnetic monopole. Then the magnetophoretic force exerted on the ball can be expressed as

$$F(x) = \frac{cx}{(x^2 + h^2)^3}, \quad (26)$$

where c and h are parameters of the platform. c comprises several physical parameters and h is the vertical distance between the virtual monopole and the horizontal plane of manipulation. These parameters were obtained by experimental identification when the force and the position were measured at the same time (to measure the force, a digital force gauge was used). The measured dataset was used afterwards to find the least square fit to the function (26) and the final prescription is

$$F(x) = \frac{-1.823x}{(x^2 + 14.37^2)^3} 10^6, \quad (27)$$

where x is measured in millimeters and value of $F(x)$ is in newtons. You may notice that the value of b is close to the radius of the ball.

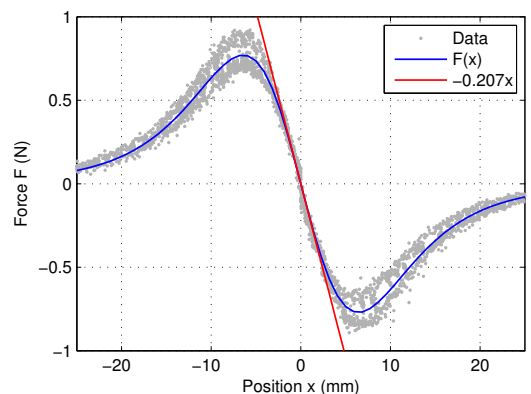


Fig. 11. Evolution of the magnetic force along the x -axis exerted on the 30 mm steel ball.

The force profile is depicted in Fig. 11. Besides this nonlinear model, the original measured data and the linearization of the force in the vicinity of the origin ($F(x) = -kx$, $k = 0.270$) are plotted here. It appears that the linearization approximates the force enough to distance around 5 mm from the center of the coil.

The dynamics of the ball is modelled using second Newton's law

$$\ddot{x} = \frac{F(x)}{m_{\text{eff}}} 10^3, \quad m_{\text{eff}} = \frac{7}{5}m, \quad (28)$$

where m_{eff} is the effective mass which also includes influence of moment of inertia of the ball. The mass of the ball m is 110 g and x is in millimeters. Therefore, if the coil is turned on, the linearized system is described as a bilinear system

$$\begin{aligned} \begin{bmatrix} \dot{x}_1(t) \\ \dot{x}_2(t) \end{bmatrix} &= \begin{bmatrix} 0 & 1 \\ 0 & 0 \end{bmatrix} \begin{bmatrix} x_1(t) \\ x_2(t) \end{bmatrix} + \begin{bmatrix} 0 & 0 \\ -\psi & 0 \end{bmatrix} \begin{bmatrix} x_1(t) \\ x_2(t) \end{bmatrix} u(t), \\ u(t) &\in \{0, 1\}, \\ \psi &= \frac{k}{m_{\text{eff}}} 10^3 = 1.344 \cdot 10^3. \end{aligned} \quad (29)$$

3.3 Controller implementation

A few implementation issues will be discussed here. Although these are not central to the key control design idea presented in the paper, they were important for a success of the experiments. First, a velocity observer needed to be designed since the direct measurement of velocity is not available and the measurement of position is rather noisy (standard deviation of 0.7 mm). Standard Kalman filter was used to accomplish this task. We incorporated the knowledge of the dependence of force on the position as a nonlinearity at the input of the filter. Needless to emphasize here that the filter is crucial for the good performance of the controller because the control law relies on the ratio between the velocity and the position; if one of them is not estimated accurately enough, the controller will not operate correctly.

The second implementation issue is that the theoretical results derived in this paper hold for the normalized model ($\psi = 1$). Therefore unscaling needs to be done by dividing the velocity by $\sqrt{\psi} = 36.7$.

The controller was implemented in Matlab/Simulink and run in External Mode utilizing Real-Time Windows Target. The sampling rate was set to 1 kHz.

3.4 Results and discussion

The experimental scenario was such that the ball was at the beginning accelerated to some reference velocity (specifically, 150 mm/s) by another controller (designed ad hoc) and when it reached the origin ($x = 0$ mm), the switching controller proposed in this paper was activated. It means that the initial condition for the experiments was zero position and some non-zero velocity. Examples of recorded variables (namely measured position, estimated position, estimated velocity, and control signal) are in Fig. 12.

You can compare the variables measured on the platform with the variables obtained by the simulation on the linear model. These values, which have been already presented, were transformed to match the not-normalized system. It means simulated velocity had to be multiplied by $\sqrt{\psi} = 36.7$ and the simulation time was divided by this factor.

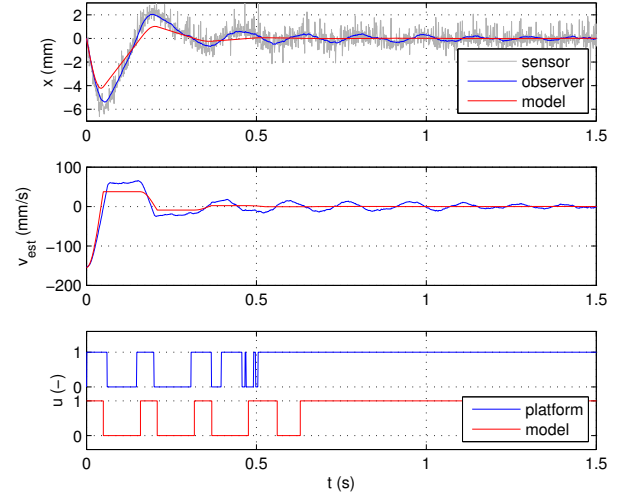


Fig. 12. Comparison of the measured values obtained with the platform and simulated with the linear model.

It is noticeable that the simulated and the measured control signal are quite similar at the beginning, but later they diverge. This difference can be partially caused by the fact that the linearized model does not match the real system with increasing distance of the ball from the coil. Namely braking at the beginning is less intensive than it is supposed to be and that is why the real system reaches further position. Nevertheless, first three pulses of the measured and the modelled control signal are quite similar. Other pulses of the control signal during the experiment are not relevant because fluctuation of the estimated position is too high to get the ball to absolute rest.

Fig. 13 provides a comparison of evolutions of the ball positions during several experiments (Video from the experiment is available at <http://youtu.be/5r4IdUrz6Sg>). It is possible to see that at the beginning they are very similar whereas later they start differing. Also clearly visible is the (natural) fact that the response of the uncontrolled system has much longer settling time. The mathematical model considered in the paper contains no damping (friction), but in reality there is one—eddy currents (Foucault currents) in the ball; the rolling friction is negligible.

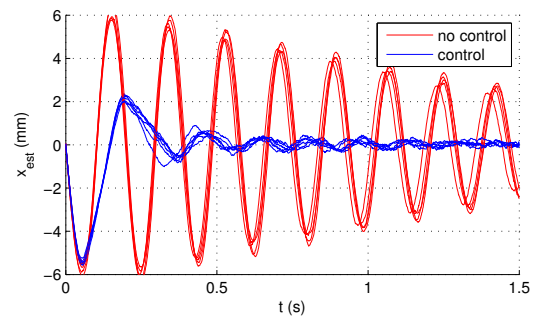


Fig. 13. Comparison of evolutions of estimated position (for several runs, just in order to assess the repeatability).

4. CONCLUSIONS

An extension of the proposed control strategy into a 2D spatial domain (plane) is straightforward. Another extension that is planned for this work is to include another source(s) of force, which can be easily realized by adding another coil(s) in the experimental magnetic setup. The resulting force field will be then composed of two or more local contributions since the *zones of influence* of the sources (coils) are overlapping. Laboratory experiments with a magnetic manipulation platform based on a planar rectangular array of coils and an iron ball rolling on top of them will be conducted, see more on *Distributed manipulation by shaping magnetic field (MagMan platform)* at <http://aa4cc.dce.fel.cvut.cz> in the corresponding section.

REFERENCES

- Betts, J.T. (2009). *Practical Methods for Optimal Control and Estimation Using Nonlinear Programming, Second Edition*. Society for Industrial & Applied Mathematics, Philadelphia, 2nd edition.
- Böhringer, K.F., Donald, B., Mihailovich, R., and MacDonald, N. (1994). A theory of manipulation and control for microfabricated actuator arrays. In *Micro Electro Mechanical Systems, 1994, MEMS '94, Proceedings, IEEE Workshop on*, 102–107. doi:10.1109/MEMSYS.1994.555606.
- Böhringer, K.F., Choset, H., and Choset, H. (2000). *Distributed manipulation*.
- Diehl, M. (2011). Numerical Optimal Control.
- Elliott, D. (2009). *Bilinear Control Systems: Matrices in Action*. Springer.
- Gorman, J.J. and Shapiro, B. (eds.) (2012). *Feedback Control of MEMS to Atoms*. Springer.
- Hargraves, C.R. and Paris, S.W. (1987). Direct trajectory optimization using nonlinear programming and collocation. *Journal of Guidance, Control, and Dynamics*, 10(4), 338–342. doi:10.2514/3.20223.
- Hurak, Z. and Zemanek, J. (2012). Feedback linearization approach to distributed feedback manipulation. In *American Control Conference (ACC), 2012*, 991–996.
- Lewis, F.L. and Syrmos, V.L. (1995). *Optimal Control*. Wiley-Interscience, 2 edition.
- Liberzon, D. (2003). *Switching in Systems and Control*. Birkhuser Boston, 2003 edition.
- Luntz, J.E., Messner, W., and Choset, H. (2001). Distributed manipulation using discrete actuator arrays. *The International Journal of Robotics Research*, 20(7), 553–583. doi:10.1177/02783640122067543.
- Murphey, T.D. and Burdick, J.W. (2004). Feedback control methods for distributed manipulation systems that involve mechanical contacts. *The International Journal of Robotics Research*, 23(7-8), 763–781. doi:10.1177/0278364904045480.
- Sun, Z. (2005). *Switched Linear Systems: Control and Design*. Springer, 1st edition.